Performance on Cognitive Broadcasting Networks Employing Fountain Codes and Maximal Ratio Transmission

Ngoc-Long NGUYEN [1], Lam-Thanh TU [2], Tan N. NGUYEN [2], Phuong-Loan T. NGUYEN [3], Quang-Sang NGUYEN [4]

[1] Faculty of Applied Sciences, Ton Duc Thang University, Ho Chi Minh City, Vietnam
[2] Communication and Signal Processing Research Group, Faculty of Electrical and Electronics Engineering, Ton Duc Thang University, 756000 Ho Chi Minh City, Vietnam
[3] Faculty of Fundamental 2, Posts and Telecommunications Institute of Technology, Ho Chi Minh City, Vietnam
[4] Science and Technology Application for Sustainable Development Research Group, Ho Chi Minh University of Transport, Ho Chi Minh City, Vietnam

nguyenngoclong@tdtu.edu.vn, tulamthanh@tdtu.edu.vn, nguyennhattan@tdtu.edu.vn, ntploan@ptithcm.edu.vn,
Corresponding author: sang.nguyen@ut.edu.vn

Submitted August 11, 2022 / Accepted November 24, 2022 / Online first December 8, 2022

Abstract. *The comprehensive performance of cognitive broadcasting networks employing Fountain codes (FC) and maximal ratio transmission (MRT) is investigated in the present paper. More precisely, the secondary transmitter (ST) employs Fountain code to effectively broadcast a common message such as a safety warning, security news, etc., to all secondary receivers (SRs) via underlay protocol of cognitive radio networks (CRNs). Different from works in the literature that are interested in studying the outage probability (OP), and the ergodic capacity of the CRNs. The present paper, on the other hand, focuses on the characteristics of the number of needed time slots to successfully deliver such a message. Particularly, we derive in closed-form expressions the cumulative distribution function (CDF), the probability mass function (PMF), and the average number of the required time slot to broadcast the message to all SRs. Additionally, we also provide the throughput of secondary networks (SNs). We point out the impact of some key parameters, i.e., the number of SRs and the number of transmit antennae at the secondary transmitter, on the performance of these considered metrics. Numerical results via the Monte-Carlo method are given to verify the accuracy of the derived framework as well as to highlight the influences of some essential parameters. Furthermore, we also compare the performance of the proposed networks with state-of-the-art and simulation results unveiling that the considered system consistently outperforms works in the literature.*

Keywords

Broadcasting networks, cognitive radio, fountain codes, maximal ratio transmission, performance analysis

1. Introduction

Cognitive radio networks (CRNs) is one of the effective solutions to facilitate spectral efficiency (SE) in wireless networks. Particularly, by permitting secondary users (SUs) to access the licensed spectra of the primary networks (PNs), CRNs, theoretically, enhances the SE and energy efficiency (EE) of the whole networks [1], [2]. To realize such networks, there are two popular protocols proposed in the literature, namely, the overlay and underlay protocols. The former allows SUs to opportunistically utilize the unoccupied resources (frequency and/or time) left by PNs. The latter, on the other hand, allows SUs to operate concurrently with PNs provided that the aggregate interference measured on primary users (PUs) is less than a predefined threshold. Compared with the overlay protocol, the underlay is preferable since SUs can operate whenever they want. To further ameliorate the SE and EE of wireless networks towards 5G-Advanced, the combinations of CRNs with other techniques are expected. One of the promising ways is to simultaneously broadcast the common information to as many as possible terminals to save energy and resources thus improving the SE and EE. However, the conventional broadcasting network suffers from a very low SE owing to the re-transmission protocol. In fact, the sender needs to re-transmit lost packets to all terminals even though only a single terminal is not able to decode these packets. To overcome this issue, one may employ the Fountain codes (FCs) that divide the message into several packets and each transmitted packet is encoded based on a random generator matrix with a huge number of coefficients [3]. On the receiver side, each receiver solely needs to collect a sufficient number of different packets to decode the message and is independent of other users thus making it a promising solution to apply to the broadcast networks.

DOI: 10.13164/re.2023.0001

The performance of the CRNs studied widely in [4–12] while the performance of FCs was investigated in [13–19]. Particularly, authors in [4] addressed the channel estimation problem in the overlay CRNs based on the state transition probability method. The results show that the proposed method outperforms the literature upto 40% relying on the setup parameters. A novel spectrum sensing algorithm for CR-based Internet-of-thing (IoT) was given in [5] to facilitate the efficiency and time sensitivity compared with other approaches. The outage performance of both primary and secondary networks in cognitive device-to-device (D2D) network was derived in the closed-form expressions in [6]. Besides, the secrecy performance of CRNs in Nakagami-*m* distribution was addressed in [7]. Authors in [8] maximized the throughput of the two-way CRNs simultaneous wireless information and power transfer (SWIPT) with the help of multiple relays. The results illustrated that the EE is a unimodal function of the signal-to-noise ratio (SNR) while the throughput is a monotonic increasing function. The impact of the imperfect channel state information (CSI) on the performance of secrecy outage probability (SOP) in CRNs was derived in [9]. The outcomes proved that by employing diversity techniques [10], the impact of imperfect CSI can be straightforwardly overcome. Duy, et al. investigated a hybrid spectrum sharing method in CRNs. More precisely, the SUs operate either in the overlay or underlay protocols depending on the quality-of-service (QoS) of the primary networks. The secure performance of non-orthogonal multiple access (NOMA) cognitive radio networks with mmWave was given in [11] while the performance of CRNs with the assistance of reconfigurable intelligent surfaces (RISs) was investigated in [12].

On the other hand, authors in [13] addressed the performance of FCs with the general Galois field ($F_q \geq 2$). The results illustrated that utilizing higher Galois fields is more beneficial as it reduces the decoding error probability. A novel design of the distributed Fountain codes was proposed to apply for the unequal protection in [14]. Hung and others studied the secrecy performance of the multiple-input and multiple-output (MIMO) systems with and without NOMA [15]. The results showed that the system employing NOMA declines the intercept probability and the number of time slots to deliver packets. Authors in [16] investigated the performance of the cooperative communications with Fountain codes in order to scale down the decoding complexity. Specifically, they studied the outage probability (OP) and the discussion of the practical application. Besides, the performance of the multi-hop cooperative transmission with FCs over Rayleigh fading was given in [17]. The combination of SWIPT and FCs was studied in [18]. Particularly, both source and relay are operated based on the harvesting energy under two protocols, time switching (TS) and power splitting (PS). The outcomes showed that the PS protocol outperforms the TS ones. A novel analog FCs was designed to apply for the short packet communications [19].

All of the above-mentioned works, nevertheless, do not consider the application of the Fountain codes into the cognitive broadcasting networks. Additionally, the transmit diversity that can significantly enhance the system reliability is ignored and the statistics of the number of required time slots to broadcast messages are missing too. The most closet work is [20] where authors also employed Fountain codes to broadcast messages to all terminals. It, however, merely equips a single antenna at the transmitter rather than multiple antennae like the current work. The main differences between [20] and the present paper are the following:

- In the present paper, the secondary transmitter (ST) is equipped with multiple antennae while ST in [20] solely equips with a single antenna. The maximal ratio transmission (MRT) is deployed to take advantage of multiple antennae at ST. As a consequence, the mathematical framework of the signal-to-interference-plus-noise-ratio (SINR) is dissimilar and more challenging. More precisely, the distribution of the sum of multiple exponential random variables (RVs) is no longer following the exponential distribution, hence, a different approach is needed to compute the success probability to decode a packet at secondary receivers (SRs) and the derived framework is obviously not the same as [20].

- In the present work, we address the performance of the average throughput of secondary networks (SNs) while [20] focuses on the energy efficiency of the SNs.

- The mathematical framework of the transmit power of ST in the present work is distinct from [20]. Particularly, direct inspection (1), we observe that it is extremely complicated and can only be computed by employing numerical computation while the framework in [20] can straightforwardly compute in the closed-form expression.

- The large-scale path-loss model adopted in the present paper is not similar to the one applied in [20].

Different from the above-mentioned works, in the present manuscript, we study the performance of the cognitive broadcasting networks by employing Fountain codes combined with the maximal ratio transmission. Particularly, the main distributions and novelties of the manuscript are summarized as follows:

- We derive in the closed-form expressions of the cumulative distribution function (CDF), probability mass function (PMF), and the expectation of the number of needed time slots to broadcast a common message to all secondary receivers.

- We compute the throughput of the secondary networks in the closed-form equation too.

- We adopt a novel transmit power method at the secondary networks which is beneficial for both SNs and PNs.
- We provide several remarks to highlight the impact of some key parameters such as the number of SRs, the number of transmit antennae, etc., on the performance of the considered metrics.
- We supply computer-based simulation results via the Monte-Carlo method to verify the accuracy of the derived mathematical framework and to figure out the behaviors of these metrics.
- We provide comparisons with state-of-the-art to highlight the advantage of the proposed FC scheme.

The remainder of the manuscript is organized as follows: Section 2 provides the system model. The main derivations and trends are given in Sec. 3. Numerical results are provided in Sec. 4. Section 5 concludes the paper.

2. System Model

In the present paper, we investigate the performance of the cognitive radio networks which is proven to be an effective way to scale up the SE of wireless networks. Particularly, let us consider a cognitive network comprising of a primary transmitter (PT) denoted by P, a primary receiver (PR) denoted by (0), a secondary transmitter denoted by S, and $\mathcal{N}$ secondary receivers as shown in Fig. 1. The ST broadcasts a common message, i.e., a safety warning, security news, etc., to all SRs by employing FC. Particularly, the ST divides the message into $\mathcal{U}$ equal length packets. Under the FC scheme, the ST keeps transmitting novel packets, and the SRs receive and decode these packets until successfully decode the message and send an acknowledgment (ACK) packet to the ST via a simple high-accuracy feedback channel [15]. In the present work, we focus on the broadcasting channel from ST to SRs, the impact of the feedback channel is left for future works. Moreover, we assume that ST broadcasts a packet per time slot for simplicity. All nodes except for the ST are equipped with one antenna while the ST is equipped with $\mathcal{K}$ antennae.

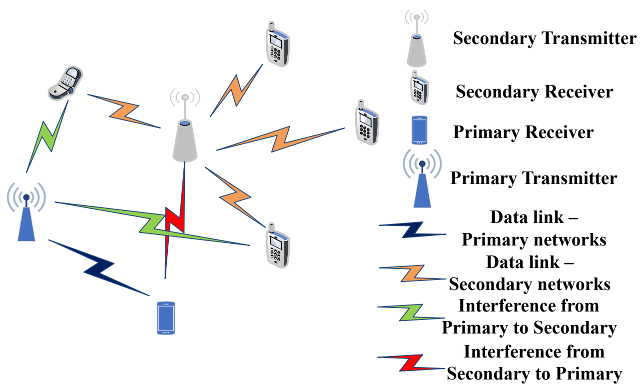

Fig. 1. Cognitive broadcasting networks.

2.1 Channel Modelling

All transmission links are subjected to both small-scale fading and large-scale path-loss. In the present work, we focus on the performance at the link level, as a result, the impact of the large-scale fading (or shadowing) is minor compared to other effects, namely, small-scale fading and large-scale path-loss. Hence, we temporarily skip it in the present work and are going to study it in future work.

Small-Scale Fading Let us denote $h_{k,n}$, $k \in \{1, \ldots, \mathcal{K}\}$, $n \in \{1, \ldots, \mathcal{N}\}$, $h_{P,0}$ as the channel coefficient from the k-th antenna of ST to the n-th SRs and from the PT to the PR and followed by a complex Gaussian distribution with zero mean and υ variance, i.e., $\mathcal{CN}(0, \upsilon)$; $f_{k,0}$, and $f_{P,n}$ are the channel coefficient from the k-th antenna of ST to PR and from the PT to the n-th SRs that follow by a complex Gaussian distribution too. The channel gain denoted by $|h_{k,n}|^2$, $|h_{k,0}|^2$, $|f_{P,n}|^2$ and $|f_{k,0}|^2$, respectively, as a result, are followed the exponential random variable. Besides, we consider the flat fading that remains constant for a time slot and changes independently between time slots.

Large-Scale Path-Loss The large-scale path-loss from node u, $u \in \{P, S\}$ to node v, $v \in \{(0), 1, \ldots, \mathcal{N}\}$ denoted by $\chi_{u,v}$ and is formulated as follows:

$$\chi_{u,v} = K_0 \big(\max\left(1, d_{u,v}\right)\big)^{\alpha} \tag{1}$$

where $d_{u,v}$ is the transmission distance from node u to node v, $K_0 = \left(\frac{4\pi}{\zeta}\right)^2$ and α are the path-loss constant and path-loss exponent, $\zeta = \frac{c}{f_c}$ is the wavelength, c is the speed of light (in [m/s]), and f_c is the carrier frequency (in [Hz]).

Remark 1 *Direct inspection* (1)*, we observe that the adopted large-scale path-loss model avoids the singular problem that is unavoidable for the unbounded path-loss model [21].*

2.2 Secondary Transmit Power Modelling

In the present paper, we adopt the transmit power model proposed by [20]. Particularly, the transmit power of ST denoted by P_S is computed as follows [20]:

$$P_S = \min\left(\max\left(0, P_A\right), P_{\max}\right), \tag{2}$$

$$P_A = \frac{\upsilon_{P,0}\chi_{S,0}P_P}{\eta_0\upsilon_{S,0}\chi_{P,0}}\left[\left(\exp\left(-\frac{\eta_0\sigma_0^2\chi_{P,0}}{\upsilon_{P,0}P_P}\right)(1-\Theta)^{-1}\right)^{1/\mathcal{K}} - 1\right].$$

Here $\min(\cdot)$, $\max(\cdot)$, and $\exp(\cdot)$ are the minimal, maximal and exponential functions. $P_{\max}$ is the maximal transmit power that ST can be transmitted owing to the hardware constraint. P_P is the transmit power of PT, σ_0^2 is the noise variance of PR and $\Theta \in [0, 1]$ is the quality-of-service threshold of the primary networks. η_0 is defined in the Appendix 1.

Proof: The proof is available in Appendix 1.

Remark 2 *It is noted that different from [20], the transmit power of ST in* (2) *is more challenging. Particularly, in the present work, the ST is equipped with multiple antennae thus the mathematical framework is more difficult since it involves the fraction square root and the exponential functions.*

2.3 Transmit Diversity

With multiple antennae at the ST, it is certain that transmit diversity techniques can be applied to improve the system reliability and in the present work, we adopt the maximal ratio transmission instead of the transmit antenna selection (TAS) in order to achieve the full diversity gain [22].

2.4 Signal-to-Interference-Plus-Noise Ratio at SRs

Under the cognitive broadcasting networks, the secondary transmitter continuously broadcasts a novel packet per time slot. The received packet at the n-th SR at the ε-th time slot is formulated as follows [20]:

$$y_n^{(\varepsilon)} = \sqrt{P_S \chi_{S,n}^{-1}} h_{S,n}^{(\varepsilon)} x_S^{(\varepsilon)} + \sqrt{P_P \chi_{P,n}^{-1}} f_{P,n}^{(\varepsilon)} x_P^{(\varepsilon)} + n_n. \quad (3)$$

Here n_n is the additive Gaussian white noise (AWGN) at the n-th SR, $x_S^{(\varepsilon)}$, $x_P^{(\varepsilon)}$ are the transmitted signals from ST and PT at the ε-th time slot and $\mathbb{E}\left\{x_S^{(\varepsilon)}\right\} = \mathbb{E}\left\{x_P^{(\varepsilon)}\right\} = 1$ where $\mathbb{E}\{\cdot\}$ is the expectation operator. Moreover, as we consider the block flat fading the superscript ε in (3) can be omitted and y_n is re-written as follows [20]:

$$y_n = \sqrt{P_S \chi_{S,n}^{-1}} h_{S,n} x_S + \sqrt{P_P \chi_{P,n}^{-1}} f_{P,n} x_P + n_n. \quad (4)$$

From (4), the signal-to-interference-plus-noise ratio at the n-th SRs denoted by SINR_n is then given as

$$\mathrm{SINR}_n = \frac{\left(P_S/\chi_{S,n}\right) \sum_{k=1}^{\mathcal{K}} \left|h_{k,n}\right|^2}{\sigma_n^2 + \left(P_P/\chi_{P,n}\right)\left|f_{P,n}\right|^2} \quad (5)$$

where $\sigma_n^2 = \sigma^2 = -174 + NF + 10\log(Bw)\,\forall n$ is the noise variance of the n-th receiver, NF (in [dB]) is the noise figure, Bw (in [Hz]) is the transmission bandwidth.

Remark 3 *Compared with [20], it is obvious that the SINR in* (5) *is far better since it is the summation of several signals thanks to multiple antennae at the transmitter.*

3. Performance Analysis

In this section, we investigate the success probability to decode a packet, the CDF, PMF, and the average number of the required time slots to successfully deliver the message to all SRs, and the throughput of the secondary system.

3.1 Success Probability to Decode a Packet at SRs

The success probability to decode a packet of the n-th SR denoted by $P_{\mathrm{suc}}(n)$ is computed as

$$\begin{aligned}
P_{\mathrm{suc}}(n) &= \Pr\{\mathrm{SINR}_n \geq \eta\} \\
&= \Pr\left\{\sum_{k=1}^{\mathcal{K}} \left|h_{k,n}\right|^2 \geq \left(\frac{\eta\chi_{S,n}\sigma^2}{P_S} + \frac{\eta P_P \chi_{S,n}}{P_S \chi_{P,n}}\left|f_{P,n}\right|^2\right)\right\} \\
&\overset{(a)}{=} \int_{x=0}^{\infty} \frac{\Gamma\left(\mathcal{K}, \frac{\eta\chi_{S,n}\sigma^2}{\upsilon_{S,n}P_S} + \frac{\eta P_P\chi_{S,n}}{\upsilon_{S,n}P_S\chi_{P,n}}x\right)}{\Gamma(\mathcal{K})} \frac{1}{\upsilon_{P,n}} \exp\left(-\frac{x}{\upsilon_{P,n}}\right) \mathrm{d}x \\
&\overset{(b)}{=} \exp\left(-\frac{\eta\chi_{S,n}\sigma^2}{\upsilon_{S,n}P_S}\right) \sum_{m=0}^{\mathcal{K}-1} \sum_{o=0}^{m} \binom{m}{o} \frac{1}{m!} \frac{\left(\sigma^2\right)^{m-o}}{\upsilon_{P,n}} \left(\frac{\eta\chi_{S,n}}{\upsilon_{S,n}P_S}\right)^m \\
&\times \left(\frac{P_P}{\chi_{P,n}}\right)^o \int_{x=0}^{\infty} x^o \exp\left(-x\left(\frac{1}{\upsilon_{P,n}} + \frac{\eta P_P \chi_{S,n}}{\upsilon_{S,n}P_S\chi_{P,n}}\right)\right) \mathrm{d}x \\
&\overset{(c)}{=} \exp\left(-\frac{\eta\chi_{S,n}\sigma^2}{\upsilon_{S,n}P_S}\right) \sum_{m=0}^{\mathcal{K}-1} \sum_{o=0}^{m} \binom{m}{o} \frac{o!}{m!} \frac{\left(\sigma^2\right)^{m-o}}{\upsilon_{P,n}} \\
&\times \left(\frac{\eta\chi_{S,n}}{\upsilon_{S,n}P_S}\right)^m \left(\frac{P_P}{\chi_{P,n}}\right)^o \left(\frac{1}{\upsilon_{P,n}} + \frac{\eta P_P\chi_{S,n}}{\upsilon_{S,n}P_S\chi_{P,n}}\right)^{-o-1} \quad (6)
\end{aligned}$$

where $\eta = 2^{R_S} - 1$ and R_S is the expected rate, $\Pr\{\cdot\}$ is the probability operator, $\Gamma(.)$ is the Gamma function [23, Eq. 8.310] and $\Gamma(.,.)$ is the upper incomplete Gamma function [23, Eq. 350.2]. (a) is held by substituting the probability density function of the random variable $\left|f_{P,n}\right|^2$ and borrowing the results from [24] that the sum of $\mathcal{K}$ independent and identical distribution (i.i.d.) exponential RVs follows a Gamma distribution. (b) is attained by employing [23, Eq. 352.4] and the binomial theorem and (c) is held by computing the integration.

Remark 4 *From* (6)*, we see that the impact of the number of antennae $\mathcal{K}$ on the performance of P_{suc} is beneficial. Particularly, P_{suc} is a monotonic increase function with respect to $\mathcal{K}$ since P_{suc} is the summation of all positive terms, thus, it is always greater than the work in [20] that has a single antenna at the ST.*

3.2 CDF of the Needed Time-Slot to Broadcast $\mathcal{U}$ Packets

The CDF of the required time-slot to successfully decode $\mathcal{U}$ packets at all SRs denoted by $F_{\mathrm{B}}(t)$, $t \geq \mathcal{U}$, is formulated as [20]:

$$F_{\mathrm{B}}(t) = \Pr\left\{\max_{n\in\{1,\mathcal{N}\}} \{X_1, \ldots, X_{\mathcal{N}}\} \leq t\right\} \overset{(a)}{=} \prod_{n=1}^{\mathcal{N}} F_{X_n}(t),$$

$$F_{X_n}(t) = \Pr\{X_n \leq t\} \overset{(b)}{=} \sum_{v=\mathcal{U}}^{t} p_{X_n}(v),$$

$$p_{X_n}(v) = \Pr\{X_n = v\} = \binom{v-1}{\mathcal{U}-1} (P_{\text{suc}}(n))^{\mathcal{U}} \times (1 - P_{\text{suc}}(n))^{t-\mathcal{U}} \overset{(c)}{=} \mathcal{I}_{P_{\text{suc}}(n)}(\mathcal{U}, t - \mathcal{U} + 1), \forall n. \quad (7)$$

Here $\mathcal{I}_x(a,b)$ is the regularized incomplete beta function [25, Eq. 8.17.2], (a) is obtained by utilizing the independent property of $\mathcal{N}$ RVs, i.e., X_n, $n \in \{1,\ldots,\mathcal{N}\}$, X_n is the number of required time-slot to successfully decode $\mathcal{U}$ packets at the n-th SR. (b) is attained by employing the definition of CDF and (c) is derived with the help of [25, Eq. 8.17.5]. $F_{X_n}(v)$, $p_{X_n}(v)$ is the CDF, PMF of the n-th SR to successfully receive $\mathcal{U}$ packets in v time-slots and follows by the negative binomial distribution.

Remark 5 *Inspecting* (7)*, it is obvious that increasing the number of SRs, $\mathcal{N}$ will simply decline the $F_B(t)$ as it is the outcome of the product of numbers between zero and one, i.e., $\mathcal{I}_{P_{suc}(n)}(\mathcal{U}, t-\mathcal{U}+1) \in [0,1]$.*

Remark 6 *There is no doubt that the regularized incomplete beta function $\mathcal{I}_{P_{suc}(n)}(\mathcal{U}, t-\mathcal{U}+1)$ is monotonically increasing with $P_{suc}(n)$. Additionally, from Remark 4, we know that $P_{suc}(n)$ under the considered MRT scheme is better than $P_{suc}(n)$ having a single antenna [20]. Hence, the CDF of the considered networks is superior to the one considered in [20].*

3.3 PMF of the Needed Time-Slot to Broadcast $\mathcal{U}$ Packets

The probability mass function of the needed time-slot to broadcast $\mathcal{U}$ packets to $\mathcal{N}$ SRs denoted by $p_{\text{B}}(t)$ is computed as follows:

$$p_{\text{B}}(t) = \Pr\left\{\max_{n\in\{1,\mathcal{N}\}} \{X_1,\ldots,X_{\mathcal{N}}\} = t\right\} \overset{(a)}{=} F_{\text{B}}(t) - F_{\text{B}}(t-1) = \prod_{n=1}^{\mathcal{N}} F_{X_n}(t) - \prod_{n=1}^{\mathcal{N}} F_{X_n}(t-1) \quad (8)$$

where (a) is obtained from the definition of the probability mass function.

Remark 7 *It is noted that if $t = \mathcal{U}$ then $F_B(t-1) = 0$ according to the definition that $t \geq \mathcal{U}$.*

3.4 Average Needed Time-Slot to Broadcast $\mathcal{U}$ Packets

In this section, we compute the average needed time-slot to broadcast $\mathcal{U}$ packets to all SRs. Let us denote $\mathcal{E}(\mathcal{U})$ as the average number of required time-slot, it then calculates as follows:

$$\mathcal{E}(\mathcal{U}) = \sum_{x=\mathcal{U}}^{\infty} x p_{\text{B}}(x) = \sum_{x=\mathcal{U}}^{\infty} x \left(\prod_{n=1}^{\mathcal{N}} F_{X_n}(t) - \prod_{n=1}^{\mathcal{N}} F_{X_n}(t-1)\right). \quad (9)$$

Remark 8 *As proven in [20], the average required time slots to broadcast $\mathcal{U}$ packets under the uncoded broadcast needs exactly $\mathcal{U}\,\mathcal{E}(1)$ time slots that are substantially greater than the FC scheme since $\mathcal{E}(\mathcal{U})$ goes up with a slower pace.*

3.5 Throughput of the Secondary Networks

The throughput of the secondary system that measures the average number of transmitted packets per second denoted by $\mathcal{TR}$ (in [packets/s]) is computed as the ratio of the number of delivered packets to the average number of needed time-slot to broadcast these packets. Mathematical speaking, $\mathcal{TR}$ is formulated as follows:

$$\mathcal{TR} = \frac{\mathcal{U}}{\mathcal{E}(\mathcal{U})}. \quad (10)$$

4. Numerical Results

Simulation results via the Monte-Carlo method are given to verify the accuracy of the derived mathematical framework as well as to identify the behaviors of these metrics with respect to some key parameters. All results are conducted by employing one of the most popular software, i.e., MATLAB. Regarding the simulator, it is employed according to the system model described in Sec. 2. Particularly, the whole simulation comprises 10^4 realizations. For each realization, the PT keeps transmitting information to the PR while the ST consistently generates a novel packet for each time slot and broadcasts to all SRs unless receiving all ACKs from $\mathcal{N}$ SRs. At the SR, they will decode every packet suffering interference from the primary networks. Each SR decodes independently and sends an ACK back to the ST. If ST does not collect all ACKs after 10^3 time slots, the ST fails to deliver the message for that realization[1]. Without loss of generality, simulation parameters are given in Tab. 1[2]. The positions of ST, PT, and PR are located at $(0,0)$ [m], $(50,50)$, and $(80,80)$, respectively. The locations of 4 SRs are $(100,0)$, $(70,-35)$, $(100,25)$, $(-60,60)$, respectively. As far as the selection of simulation parameters is concerned,

[1]For the reproducible research, we have uploaded the source codes at https://drive.google.com/drive/folders/1bXri77EZn7ALl0NKqbg6OvOUfMO4a30X?usp=share_link. We kindly invite all interested readers to visit it.

[2]Here, f_c is chosen to 2.1 GHz in order to align with the current 4G systems. However, it is emphasized that our system works well with all sub-6GHz carrier frequencies.

Full name	**Notations**	**Values** [unit]
Carrier frequency	f_c	2.1 [GHz]
Transmission bandwidth	Bw	5 [MHz]
Path-loss exponent	α	3.75
Noise figure	NF	6 [dB]
Expected rate	$R_S = R_P$	1 [bits/s/Hz]
QoS of primary networks	Θ	0.1
Total transmit power	P_{tot}	30 [dBm]
Transmit power of PT	P_P	20 [dBm]
Number of ST antennae	$\mathcal{K}$	4
Number of sent packets	$\mathcal{U}$	4 [packets]
Number of SRs	$\mathcal{N}$	4

Tab. 1. Simulation parameters.

it is worth pointing out that the transmit power of the PT and the maximal transmit power of ST are still in the transmission range of both macro and micro cells [26].

Figures 2, 3 stretch the behaviors of the CDF, the PMF, the average number of needed time-slot, and the throughput of the secondary system with respect to the expected rate R_S. First, we observe a good match between the derived mathematical framework and the Monte-Carlo simulations. Second, it is no doubt that increasing R_S will decline the CDF of the required time slots. The main reason is that increasing R_S obviously reduces the P_{suc} of all SRs, it leads to the decreases of the regularized incomplete beta function and the CDF too. Regarding the PMF, it is a unimodal function with respect to the R_S. It can also be directly explained from (7). Additionally, we also see that increasing the transmit power at PT slightly improves the performance of the CDF.

Figure 3(a) investigates the impact of R_S on the performance of $\mathcal{E}(\mathcal{U})$. We observe that when R_S is relatively small, $\mathcal{E}(\mathcal{U})$ is fairly small too and when R_S goes up, $\mathcal{E}(\mathcal{U})$ increases exponentially. The rationale behind this phenomenon is that all SRs can straightforwardly decode packets when R_S is small. On the other hand, all SRs is hard to decode packets when $R_S \gg 1$ thus, the average number of required time-slot goes up dramatically. Besides, the throughput of the secondary networks is a monotonic decreasing function with R_S. Particularly, when $R_S = 1$, the throughput is approximately 1 while $R_S = 3$ the $\mathcal{TR}$ has already approaching zero regardless of P_P.

The impact of the transmit power of the PT, P_P on the performance of the CDF, PMF, $\mathcal{E}(\mathcal{U})$, and $\mathcal{TR}$ is given in Figs. 4 and 5. In Fig. 4(a), we experience that the CDF starts increasing until reaching its peak, it then declines and reaches zero when $P_P \gg 1$. The principal reason is following: when P_P is small, ST has to stop transmitting in order to guarantee the QoS of primary networks, when P_P keeps increasing, the ST starts broadcasting and both primary and secondary networks are beneficial since the CDF is improved and the QoS of PNs is secured too. Nevertheless, when P_S approaches its hardware limitations, P_{max}, increasing P_P will be harmful to the SNs thus, SRs can not decode packets sent by ST and CDF plummets. Figure 4(b) plots the behaviors of PMF as a function of P_P with different values of $\mathcal{K}$. We see that there are two peaks of PMF instead of one like Fig. 2(b).

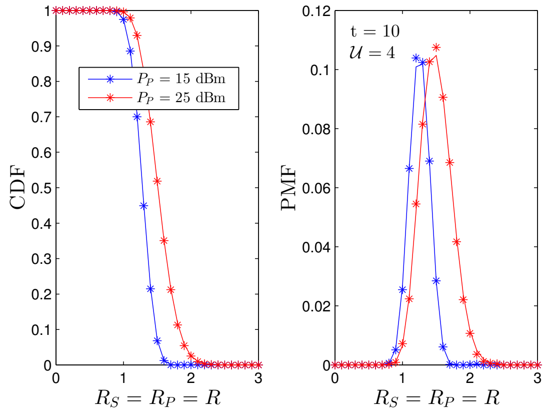

Fig. 2. CDF and PMF vs. $R_S = R_P = R$ with various values of P_P. Solid lines are plotted from (7) and (8). Markers are from Monte-Carlo simulations. $Bw = 5$ MHz, $f_c = 2.1$ GHz, $\alpha = 3.75$, $NF = 6$ dB, $\Theta = 0.1$, $P_{tot} = 30$ dBm, $\mathcal{K} = 4$, $\mathcal{U} = 4$ and $\mathcal{N} = 4$.

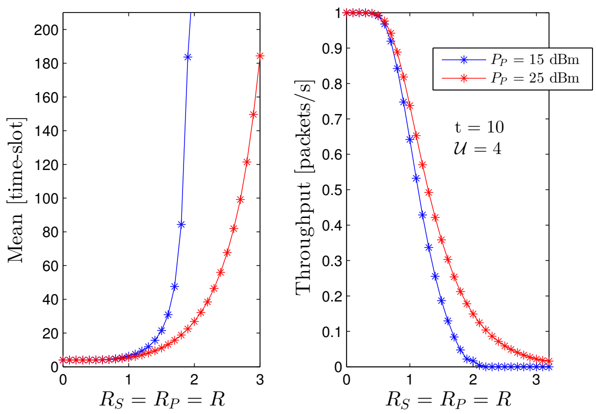

Fig. 3. Average and throughput vs. $R_S = R_P = R$ with various values of P_P. Solid lines are plotted from (9) and (10). Markers are from Monte-Carlo simulations. $Bw = 5$ MHz, $f_c = 2.1$ GHz, $\alpha = 3.75$, $NF = 6$ dB, $\Theta = 0.1$, $P_{tot} = 30$ dBm, $\mathcal{K} = 4$, $\mathcal{U} = 4$ and $\mathcal{N} = 4$.

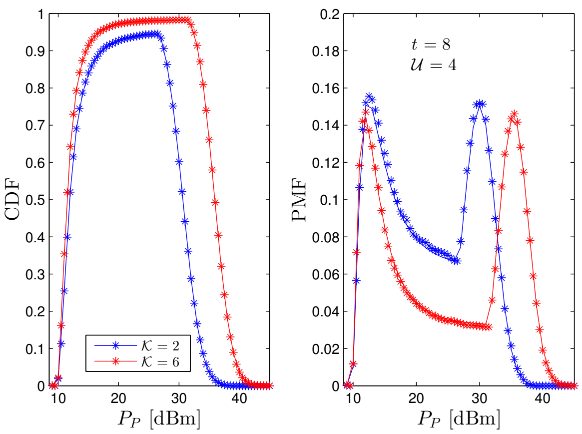

Fig. 4. CDF and PMF vs. P_P with various values of $\mathcal{K}$. Solid lines are plotted from (7) and (8). Markers are from Monte-Carlo simulations. $Bw = 5$ MHz, $f_c = 2.1$ GHz, $\alpha = 3.75$, $NF = 6$ dB, $R_S = R_P = 1$ bits/s/Hz, $\Theta = 0.1$, $P_{tot} = 30$ dBm, $\mathcal{U} = 4$ and $\mathcal{N} = 4$.

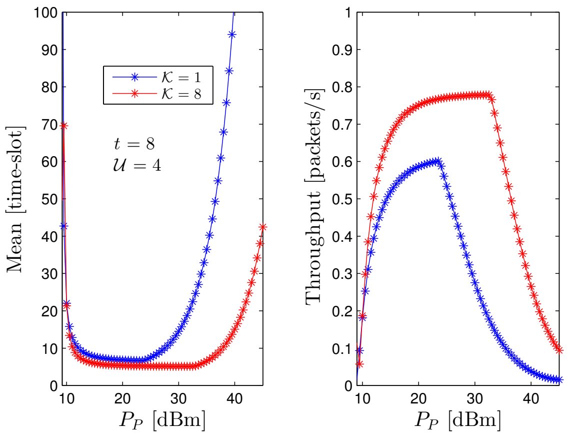

Fig. 5. Average and throughput vs. P_P with various values of $\mathcal{K}$. Solid lines are plotted from (9) and (10). Markers are from Monte-Carlo simulations. $Bw = 5$ MHz, $f_c = 2.1$ GHz, $\alpha = 3.75$, $NF = 6$ dB, $R_S = R_P = 1$ bits/s/Hz, $\Theta = 0.1$, $P_{tot} = 30$ dBm, $\mathcal{U} = 4$ and $\mathcal{N} = 4$.

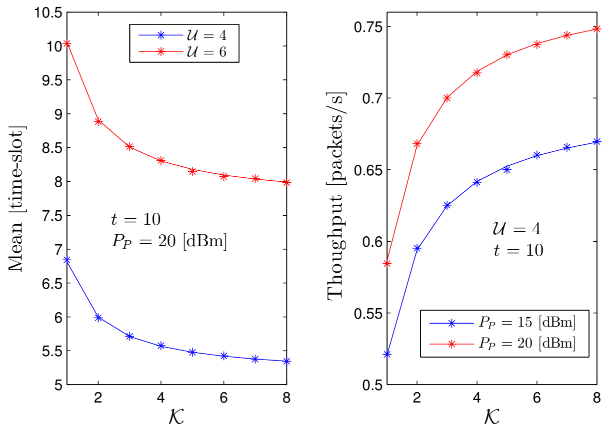

Fig. 7. Average and throughput vs. $\mathcal{K}$ with different values of P_P. Solid lines are plotted from (9) and (10). Markers are from Monte-Carlo simulations. $Bw = 5$ MHz, $f_c = 2.1$ GHz, $\alpha = 3.75$, $NF = 6$ dB, $R_S = R_P = 1$ bits/s/Hz, $\Theta = 0.1$, $P_{tot} = 30$ dBm, and $\mathcal{N} = 4$.

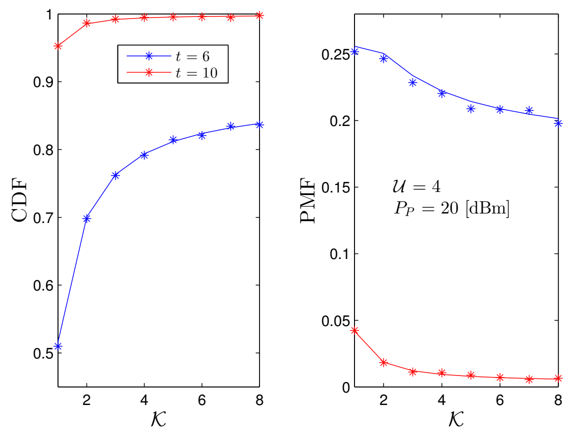

Fig. 6. CDF and PMF vs. $\mathcal{K}$ with different values of t. Solid lines are plotted from (7) and (8). Markers are from Monte-Carlo simulations. $Bw = 5$ MHz, $f_c = 2.1$ GHz, $\alpha = 3.75$, $NF = 6$ dB, $R_S = R_P = 1$ bits/s/Hz, $\Theta = 0.1$, $P_{tot} = 30$ dBm, $P_P = 20$ dBm, $\mathcal{U} = 4$ and $\mathcal{N} = 4$.

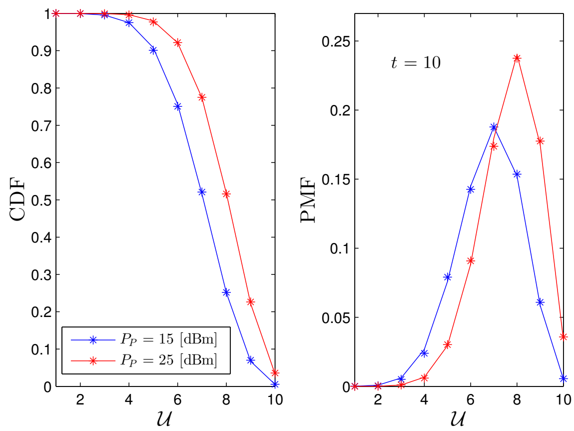

Fig. 8. CDF and PMF vs. $\mathcal{U}$ with several values of P_P. Solid lines are plotted from (7) and (8). Markers are from Monte-Carlo simulations. $Bw = 5$ MHz, $f_c = 2.1$ GHz, $\alpha = 3.75$, $NF = 6$ dB, $R_S = R_P = 1$ bits/s/Hz, $\Theta = 0.1$, $P_{tot} = 30$ dBm, $\mathcal{K} = 4$, and $\mathcal{N} = 4$.

In Fig. 5(a), the performance of the $\mathcal{E}(\mathcal{U})$ concerning P_P has a contrary trend with the CDF that it begins with a drastic drop to approximately 7 time-slot followed by a slight decline, it then scale up to a huge number. Besides, Figure 5(b) shows that the larger the number of transmit antennae the better the throughput. Moreover, $\mathcal{TR}$ has the same trend as the CDF too.

Figures 6 and 7 provide the detailed performance of the CDF, PMF, the average number of needed time-slot to broadcast $\mathcal{U}$ packets to all SRs as well as the throughput of the secondary networks regarding the number of transmit antennae at ST, $\mathcal{K}$. It is certain that raising up $\mathcal{K}$ benefits all metrics. Specifically, the CDF and the throughput simply ameliorate with the increase of $\mathcal{K}$ while the PMF and the expectation go down.

The influences of the number of packets, $\mathcal{U}$, on the performance of all metrics are given in Figs. 8 and 9. Particularly, increasing $\mathcal{U}$ while fixing t will decrease the CDF. The explanation is the following: increasing $\mathcal{U}$ means raising up the number of transmitted packets while the number of allowed time-slot t to successfully broadcast these packets is fixed. As a result, the probability of successfully delivering these packets will go down. The PMF is a unimodal function of $\mathcal{U}$, this can be explained by employing the property of the binomial coefficient in (7). Besides, in Fig. 9(a), it is evident that $\mathcal{E}(\mathcal{U})$ climbs up with $\mathcal{U}$ since it requires more time-slot to deliver more packets. The $\mathcal{TR}$ slightly enhances with $\mathcal{U}$ and is shown in Fig. 9(b).

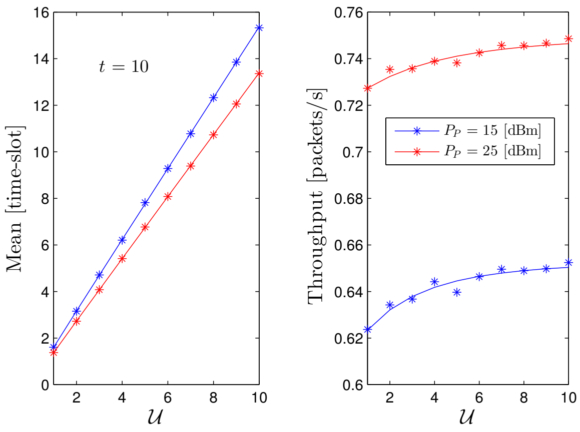

Fig. 9. Average and throughput vs. $\mathcal{U}$ with several values of P_P. Solid lines are plotted from (9) and (10). Markers are from Monte-Carlo simulations. $Bw = 5$ MHz, $f_c = 2.1$ GHz, $\alpha = 3.75$, $NF = 6$ dB, $R_S = R_P = 1$ bits/s/Hz, $\Theta = 0.1$, $P_{\text{tot}} = 30$ dBm, $\mathcal{K} = 4$, and $\mathcal{N} = 4$.

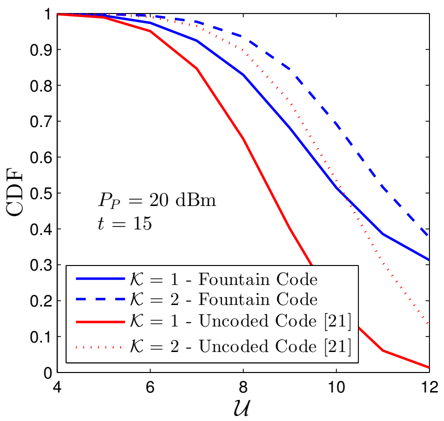

Fig. 10. CDF vs. $\mathcal{U}$ with several values of $\mathcal{K}$ and schemes. All curves are from Monte-Carlo simulations. $Bw = 5$ MHz, $f_c = 2.1$ GHz, $\alpha = 3.75$, $NF = 6$ dB, $R_S = R_P = 1$ bits/s/Hz, $\Theta = 0.1$, $P_{\text{tot}} = 30$ dBm, and $\mathcal{N} = 4$.

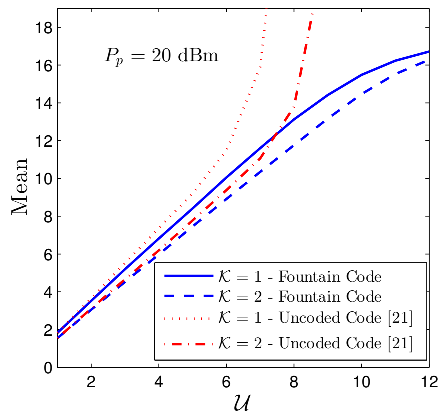

Fig. 11. Average vs. $\mathcal{U}$ with several values of $\mathcal{K}$ and schemes. All curves are from Monte-Carlo simulations. $Bw = 5$ MHz, $f_c = 2.1$ GHz, $\alpha = 3.75$, $NF = 6$ dB, $R_S = R_P = 1$ bits/s/Hz, $\Theta = 0.1$, $P_{\text{tot}} = 30$ dBm, $\mathcal{K} = 4$, and $\mathcal{N} = 4$.

Figure 10 addresses the performance of the CDF with respect to the number of transmitted packets $\mathcal{U}$ under different values of the number of transmit antennae $\mathcal{K}$ and two schemes, i.e., Fountain Code broadcast and uncoded broadcast (UB) in [20][3]. It is noted that all curves are plotted based on Monte-Carlo simulations. We observe that the UB scheme always underperforms the proposed FC scheme. Additionally, we also observe that the FC scheme for $\mathcal{K} = 1$ is even better than the UB scheme with $\mathcal{K} = 2$ when $\mathcal{U}$ is large. It means that the FC scheme is superior to its counterpart.

Figure 11 illustrates the average number of required time slots to broadcast $\mathcal{U}$ packets under both schemes, FC and UB, respectively. It is evident that the FC requires fewer time slots than the UB. Moreover, when the number of sent packets goes large, the needed time slots for the UB remarkably increase and may approach infinity. The FC scheme, on the other hand, goes up with a slower pace. Thus, it confirms again that the considered FC consistently outperforms the UB scheme in the literature.

5. Conclusions

The performance of the cognitive broadcasting networks employing FC and MRT technique was investigated in this work. Particularly, we studied the CDF, PMF, and expectation of the number of required time slots to broadcast an arbitrary packet to all secondary receivers were computed in the closed-form expressions. Additionally, we also provided the throughput of the secondary networks and the success probability to decode a packet without error. Furthermore, the impact of some key parameters on the performance of these metrics was discussed too. Finally, numerical results were given to clarify the correctness of the proposed mathematical framework. Regarding the extensions, the manuscript can be extended in several directions such as employing relaying and/or multi-hop communications to enhance the system reliability [27], [24], utilizing tools from stochastic geometry to better capture the randomness of wireless networks [28], adopting long-range (LoRa) networks to take advantage of lower power long-range transmission [29], [30], and deep learning to exploit the power of data-driven [31].

References

[1] ZHANG, Z., WU, Q., WANG, J. Energy-efficient power allocation strategy in cognitive relay networks. *Radioengineering*, 2012, vol. 21, no. 3, p. 809–814. ISSN: 1805-9600

[2] FERDOUS, N., AHMED, M., MATIN, M. A. et al. Efficient algorithm for power allocation in relay-based cognitive radio network. *Radioengineering*, 2011, vol. 20, no. 4, p. 946–951. ISSN: 1805-9600

[3] Here, [20] is selected to make the comparisons with the current work because it is the closest one and is also one of the latest works published in this topic.

[3] ZHENG, Z., YUAN, L., FANG, F. Performance analysis of fountain coded non-orthogonal multiple access with finite blocklength. *IEEE Wireless Communications Letters*, 2021, vol. 10, no. 8, p. 1752–1756. DOI: 10.1109/LWC.2021.3078811

[4] LI, W., SHENTU, G., GAO, X. Estimation of primary channel mean period based on state transition probability in cognitive radio. *IEEE Access*, 2022, vol. 10, p. 52410–52417. DOI: 10.1109/ACCESS.2022.3175852

[5] IDREES, Z., USMAN, M., GELANI, H. E., et al. Fast and robust spectrum sensing for cognitive radio enabled IoT. *IEEE Access*, 2021, vol. 9, p. 165996–166007. DOI: 10.1109/ACCESS.2021.3133336

[6] NGUYEN, N. T., NGUYEN, V. S., NGUYEN, H. G., et al. On the performance of underlay device-to-device communications. *Sensors*, 2022, vol. 22, no. 4, p. 1–21. DOI: 10.3390/s22041456

[7] NGUYEN, N. P., TU, L.-T., DUONG, Q. T. Secure communications in cognitive underlay networks over Nakagami-m channel. *Physical Communications*, 2017, vol. 25, no. 2, p. 610–618. DOI: 10.1016/j.phycom.2016.05.003

[8] PRATHIMA, A., GURJAR, D. S., NGUYEN, H. H., et al. Performance analysis and optimization of bidirectional overlay cognitive radio networks with hybrid-SWIPT. *IEEE Transactions on Vehicular Technology*, 2020, vol. 69, no. 11, p. 13467–13481. DOI: 10.1109/TVT.2020.3029067

[9] SINGH, A., BHATNAGAR, M. R., MALLIK, R. K. Secrecy outage performance of SWIPT cognitive radio network with imperfect CSI. *IEEE Access*, 2020, vol. 8, p. 3911–3919. DOI: 10.1109/ACCESS.2019.2962382

[10] TU, L.-T., DI RENZO, M., COON, J. P. System-level analysis of receiver diversity in SWIPT-enabled cellular networks. *Journal of Communications and Networks*, 2016, vol. 18, no. 6, p. 926–937. DOI: 10.1109/JCN.2016.000127

[11] SONG, Y., YANG, W., XIANG, Z., et al. Research on cognitive power allocation for secure millimeter-wave NOMA networks. *IEEE Transactions on Vehicular Technology*, 2020, vol. 69, no. 11, p. 13424–13436. DOI: 10.1109/TVT.2020.3027868

[12] XU, D., YU, X., SUN, Y., et al. Resource allocation for IRS-assisted full-duplex cognitive radio systems. *IEEE Transactions on Communications*, 2020, vol. 68, no. 12, p. 7376–7394. DOI: 10.1109/TCOMM.2020.3020838

[13] LIVA, G., PAOLINI, E., CHIANI, M. Performance versus overhead for fountain codes over Fq. *IEEE Communications Letters*, 2010, vol. 14, no. 2, p. 178–180. DOI: 10.1109/LCOMM.2010.02.092080

[14] SEJDINOVIC, D., PIECHOCKI, R., DOUFEXI, A., et al. Decentralised distributed fountain coding: Asymptotic analysis and design. *IEEE Communications Letters*, 2010, vol. 14, no. 1, p. 42–44. DOI: 10.1109/LCOMM.2010.01.091541

[15] DANG, T. H., TRAN, T. D., TRAN, T. P., et al. Performance comparison between fountain codes-based secure MIMO protocols with and without using non-orthogonal multiple access. *Entropy*, 2019, vol. 21, no. 10, p. 1–23. DOI: 10.3390/e21100982

[16] LIU, X., LIM, T. J. Fountain codes over fading relay channels. *IEEE Transactions on Wireless Communications*, 2009, vol. 8, no. 6, p. 3278–3287. DOI: 10.1109/TWC.2009.081102

[17] TRAN, T. D., ANPALAGAN, A., KONG, H. Y. Multi-hop cooperative transmission using fountain codes over Rayleigh fading channels. *Journal of Communications and Networks*, 2012, vol. 14, no. 3, p. 267–272. DOI: 10.1109/JCN.2012.6253087

[18] DI, X., XIONG, K., FAN, P. et al. Simultaneous wireless information and power transfer in cooperative relay networks with rateless codes. *IEEE Transactions on Vehicular Technology*, 2017, vol. 66, no. 4, p. 2981–2996. DOI: 10.1109/TVT.2016.2588441

[19] LIM, W. J., ABBAS, R., LI, Y., et al. Analysis and design of analog fountain codes for short packet communications. *IEEE Transactions on Vehicular Technology*, 2021, vol. 70, no. 12, p. 12662–12674. DOI: 10.1109/TVT.2021.3118792

[20] TU, L.-T., NGUYEN, N. T., TRAN, T. D., et al. Broadcasting in cognitive radio networks: A fountain codes approach. *IEEE Transactions on Vehicular Technology*, 2022, vol. 71, no. 10, p. 11289–11294. DOI: 10.1109/TVT.2022.3188969

[21] TU, L.-T., DI RENZO, M., COON, P. System-level analysis of SWIPT MIMO cellular networks. *IEEE Communications Letters*, 2016, vol. 20, no. 10, p. 2011–2014. DOI: 10.1109/LCOMM.2016.2590424

[22] NGUYEN, Q. S., KONG, H. Y. Generalized diversity combining of energy harvesting multiple antenna relay networks: Outage and throughput performance analysis. *Annals of Telecommunications*, 2016, vol. 71, no. 5, p. 265–277. DOI: 10.1007/s12243-016-0508-9

[23] GRADSHTEYN, I. S., RYZHIK, I. M. *Table of Integrals, Series, and Products*. 7th ed., Oxford (UK): Elsevier/Academic Press, 2007. ISBN: 9780080471112

[24] NGUYEN, N. T., TRAN, T. P., NGUYEN, H. S., et al. On the performance of a wireless powered communication system using a helping relay. *Radioengineering*, 2017, vol. 26, no. 3, p. 860–868. DOI: 10.13164/re.2017.0860

[25] DIGITAL LIBRARY OF MATHEMATICAL FUNCTIONS: DLMF. *Incomplete Gamma and Related Functions*. [Online] Cited 2022-08-02. Available at: https://dlmf.nist.gov/8.17

[26] AUER, G., GIANNINI, V., DESSET, C., et al. How much energy is needed to run a wireless network? *IEEE Wireless Communications*, 2011, vol. 18, no. 5, p. 40–49. DOI: 10.1109/MWC.2011.6056691

[27] NGUYEN, N. T., TRAN, T. D., LUU, G. T., et al. Energy harvesting-based spectrum access with incremental cooperation, relay selection and hardware noises. *Radioengineering*, 2017, vol. 26, no. 1, p. 240–250. DOI: 10.13164/re.2017.0240

[28] DI RENZO, M., TU, L. T., ZAPPONE, A., et al. A tractable closed-form expression of the coverage probability in Poisson cellular networks. *IEEE Wireless Communications Letters*, 2018, vol. 8, no. 1, p. 249–252. DOI: 10.1109/LWC.2018.2868753

[29] SIMKA, M., POLAK, L. On the RSSI-based indoor localization employing LoRa in the 2.4 GHz ISM band. *Radioengineering*, 2022, vol. 31, no. 1, p. 135–143. DOI: 10.13164/re.2022.0135

[30] POLAK, L., PAUL, F., SIMKA, M., et al. On the interference between LoRa and bluetooth in the 2.4 GHz unlicensed band. In *32nd International Conference Radioelektronika (RADIOELEKTRONIKA)*. Kosice (Slovakia), 2022, p. 1–4. DOI: 10.1109/radioelektronika54537.2022.9764912

[31] TU, L. T., BRADAI, A., AHMED, O. B., et al. Energy efficiency optimization in LoRa networks - A deep learning approach. *IEEE Transactions on Intelligent Transport Systems*, *Early Access*, p. 1–13. DOI: 10.1109/TITS.2022.3183073

Appendix A: Proof of Equation (2)

This section provides the detail derivation of (2). Let us begin with the QoS requirement of the primary networks that the outage probability denoted by $\mathrm{OP}_{\mathrm{PN}}$ must be less than Θ where the OP of the primary networks is given below

$$
\begin{aligned}
&\mathrm{OP_{PN}} = \Pr\left\{\mathrm{SINR_{PR}} \le \eta_0 = 2^{R_P} - 1\right\} \\
&= \Pr\left\{\left|h_{P,0}\right|^2 \le \frac{\eta_0\sigma^2\chi_{P,0}}{P_P} + \frac{\eta_0 P_S \chi_{P,0}}{\chi_{S,0}P_P}\sum_{k=1}^{\mathcal{K}}\left|f_{k,0}\right|^2\right\} \\
&= \int_{i_0=0}^{\infty}\left(1 - \exp\left(-\frac{\eta_0\sigma^2\chi_{P,0}}{\upsilon_{P,0}P_P} - \frac{\eta_0\chi_{P,0}P_S}{\upsilon_{P,0}\chi_{S,0}P_P}i_0\right)\right) f_{I_0}(i_0)\,\mathrm{d}i_0 \\
&= 1 - \exp\left(-\frac{\eta_0\sigma^2\chi_{P,0}}{\upsilon_{P,0}P_P}\right) M_{I_0}\left(\frac{\eta_0\chi_{P,0}P_S}{\upsilon_{P,0}\chi_{S,0}P_P}\right) \\
&= 1 - \exp\left(-\frac{\eta_0\sigma^2\chi_{P,0}}{\upsilon_{P,0}P_P}\right)\left(1 + \frac{\eta_0\upsilon_{S,0}\chi_{P,0}P_S}{\upsilon_{P,0}\chi_{S,0}P_P}\right)^{-\mathcal{K}} \qquad \text{(A1)}
\end{aligned}
$$

where $\mathrm{SINR_{PR}} = \frac{(P_P/\chi_{P,0})\left|h_{P,0}\right|^2}{\sigma^2 + (P_S/\chi_{S,0})\sum_{k=1}^{\mathcal{K}}\left|f_{k,0}\right|^2}$ is the SINR at the primary receiver, $I_0 = \sum_{k=1}^{\mathcal{K}}\left|f_{k,0}\right|^2$ is the interference at the primary receiver from the secondary networks, $M_{I_0}(s)$ is the moment generating function (MGF) of the RV I_0.

Having obtained the OP of the PN, we are ready to compute P_{A} as follows:

$$
\begin{aligned}
&\mathrm{OP_{PN}} \le \Theta \\
&\Leftrightarrow 1 - \exp\left(-\frac{\eta_0\sigma^2\chi_{P,0}}{\upsilon_{P,0}P_P}\right)\left(1 + \frac{\eta_0\upsilon_{S,0}\chi_{P,0}P_S}{\upsilon_{P,0}\chi_{S,0}P_P}\right)^{-\mathcal{K}} \le \Theta \\
&\Leftrightarrow \exp\left(-\frac{\eta_0\sigma^2\chi_{P,0}}{\upsilon_{P,0}P_P}\right)(1-\Theta)^{-1} \ge \left(1 + \frac{\eta_0\upsilon_{S,0}\chi_{P,0}P_S}{\upsilon_{P,0}\chi_{S,0}P_P}\right)^{\mathcal{K}} \\
&\Leftrightarrow P_S \le P_{\mathrm{A}} = \frac{\upsilon_{P,0}\chi_{S,0}P_P}{\eta_0\upsilon_{S,0}\chi_{P,0}} \\
&\times\left[\left(\exp\left(-\frac{\eta_0\sigma^2\chi_{P,0}}{\upsilon_{P,0}P_P}\right)(1-\Theta)^{-1}\right)^{1/\mathcal{K}} - 1\right]. \qquad \text{(A2)}
\end{aligned}
$$

To maximize the benefits of both secondary and primary networks, P_S in (A2) is set to its maximum, $P_S = P_{\mathrm{A}}$. Finally, by considering the constraint of the hardware limitations as well as the QoS of the primary networks. P_S is given in (2). Q.E.D.

About the Authors ...

Ngoc-Long NGUYEN was born in Vietnam, in August 1973. He received the B.S. and M.S. degrees in Electric Physics from the University of Science, Vietnam, and his Ph.D. degree in Telecommunications from Technical University of Ostrava, Czech Republic in 2021. He is currently a Lecturer with the Faculty of Applied Sciences, Ton Duc Thang University. His research interests include applied electronics, wireless communication, NOMA, cognitive radio, and energy harvesting.

Lam-Thanh TU received the B.Sc. degree in Electronics and Telecommunications Engineering from the Ho Chi Minh City University of Technology, Vietnam, in 2009, the M.Sc. degree in Telecommunications Engineering from the Posts and Telecommunications Institute of Technology, Vietnam, in 2014, and the Ph.D. degree from the Laboratory of Signals and Systems, Paris-Saclay University, Paris, France, in 2018. From 2015 to 2018, he was with the French National Center for Scientific Research (CNRS), Paris, as an Early Stage Researcher of the European-funded Project H2020 ETN-5Gwireless. From 2019 to 2021, he was with the Institute Xlim, University of Poitiers, Poitiers, France, as a Postdoc Research Fellow. He is currently with the Department of Telecommunications, Ton Duc Thang University, Ho Chi Minh City, Vietnam. He was an IEEE Transactions on Communications exemplary reviewer for 2016 and a recipient of the 2017 IEEE SigTelCom Best Paper Award. He was an Assistant project manager of the H2020 MCSA 5Gwireless and 5Gaura projects. His research interests include stochastic geometry, LoRa networks, physical layer security, energy harvesting, and machine learning applications for wireless communications.

Tan N. NGUYEN was born in 1986 in Nha Trang City, Vietnam. He received a BS degree in Electronics in 2008 from Ho Chi Minh University of Natural Sciences and an MS degree in Telecommunications Engineering in 2012 from Vietnam National University. He received a Ph.D. in Communications Technologies in 2019 from the Faculty of Electrical Engineering and Computer Science at VSB - Technical University of Ostrava, Czech Republic. He joined the Faculty of Electrical and Electronics Engineering of Ton Duc Thang University, Vietnam, in 2013, and since then has been lecturing. His major interests are cooperative communications, cognitive radio, physical layer security and signal processing.

Phuong-Loan T. NGUYEN was born in Da Nang province. In 2006, she received her master's degree from the HCM University of Natural Sciences. Her research interests are telecommunication and optoelectronics. She has worked at the Faculty of Fundamental 2, Posts and Telecommunications Institute of Technology, Ho Chi Minh City, Vietnam.

Quang-Sang NGUYEN (Corresponding author: sang.nguyen@ut.edu.vn) received the B.E. degree from Ho Chi Minh City University of Transport, Ho Chi Minh City, Vietnam, in 2010, the M.E. degree from Ho Chi Minh City University of Technology, Ho Chi Minh City, in 2013, and the Ph.D. degree in Electrical Engineering from the University of Ulsan, South Korea, in 2017. From January 2017 to June 2017, he was a Postdoctoral Research Fellow with Queen's University Belfast, Belfast, U.K. From June 2017 until May 2021, he has been a Lecturer with Duy Tan University, Ho Chi Minh City. Since May 2021, He is a Head of Science of International Cooperation Department, as well as a lecturer with Ho Chi Minh City University of Transport. His major research interests are: cooperative communication, cognitive radio network, physical layer security, energy harvesting, non-orthogonal multiple access, and artificial intelligence.